Semaphorin 5A suppresses the proliferation and migration of lung adenocarcinoma cells

PIN-HAO KO[1*], GOVINDA LENKA[1,8*], YU-AN CHEN[2], ERIC Y. CHUANG[2,3], MONG-HSUN TSAI[2,4], YUH-PYNG SHER[5-7] and LIANG-CHUAN LAI[1,2]

[1]Graduate Institute of Physiology, College of Medicine, National Taiwan University, Taipei 10051; [2]Bioinformatics and Biostatistics Core, Center of Genomic and Precision Medicine, National Taiwan University, Taipei 10055; [3]Graduate Institute of Biomedical Electronics and Bioinformatics, National Taiwan University, Taipei 10617; [4]Institute of Biotechnology, National Taiwan University, Taipei 10672; [5]Graduate Institute of Clinical Medical Science and [6]Graduate Institute of Biomedical Sciences, China Medical University; [7]Center for Molecular Medicine, China Medical University Hospital, Taichung 40402, Taiwan, R.O.C.

Received May 30, 2019; Accepted November 13, 2019

DOI: 10.3892/ijo.2019.4932

Abstract. Semaphorin 5A (SEMA5A), a member of the semaphorin family, plays an important role in axonal guidance. Previously, the authors identified another possible role of SEMA5A as a prognostic biomarker for non-smoking women with lung adenocarcinoma in Taiwan, and this phenomenon has been validated in other ethnic groups. However, the functional significance of SEMA5A in lung adenocarcinoma remains unclear. Therefore, we assessed the function of SEMA5A in three lung adenocarcinoma cell lines in this study. Kaplan-Meier Plotter for lung cancer was conducted for survival analyses. Reverse transcription-quantitative PCR (RT-qPCR) and western blot analysis were performed to investigate the expression and post-translational regulation of SEMA5A in lung adenocarcinoma cell lines. A pre-designed PyroMark CpG assay and 5-aza-2'-deoxycytidine treatment were used to measure the methylation levels of *SEMA5A*. The biological functions of lung adenocarcinoma cells overexpressing *SEMA5A* were investigated by microarrays, and validated both *in vitro* (proliferation, colony formation and migration assays) and *in vivo* (tumor xenografts) experiments. The results revealed that the hypermethylation of *SEMA5A* and the cleavage of the extracellular domain of SEMA5A were responsible for the downregulation of the *SEMA5A* levels in lung adenocarcinoma cells (A549 and H1299) as compared to the normal controls. Functional analysis of *SEMA5A*-regulated genes revealed that they were involved in cellular growth and proliferation. The overexpression of *SEMA5A* in A549 and H1299 cells significantly decreased the proliferation ($P<0.01$), colony formation ($P<0.001$) and migratory ability ($P<0.01$) of the cells. The suppressive effects of *SEMA5A* on the proliferative and migratory ability of the cells were also observed in both *in vitro* and *in vivo* experiments using brain metastatic Bm7 lung adenocarcinoma cells. On the whole, the findings of this study suggest a suppressive role for SEMA5A in lung adenocarcinoma involving the inhibition of the proliferation and migration of lung transformed cells.

Correspondence to: Professor Liang-Chuan Lai, Graduate Institute of Physiology, College of Medicine, National Taiwan University, Taipei 10051, Taiwan, R.O.C.
E-mail: llai@ntu.edu.tw

Professor Yuh-Pyng Sher, Graduate Institute of Biomedical Sciences, China Medical University, Taichung 40402, Taiwan, R.O.C.
E-mail: ypsher@mail.cmu.edu.tw

Present address: [8]Laboratory of Genetic Medicine and Immunology, Weill Cornell Medicine-Qatar, Qatar Foundation-Education City, Doha 24144, Qatar

[*]Contributed equally

Key words: semaphorin 5A, lung adenocarcinoma, proliferation, migration

Introduction

Lung carcinoma, which is caused by both genetic and environmental factors, is the leading cause (18%) of cancer-related mortality worldwide (1,2). Non-small cell lung cancer (NSCLC), such as large cell carcinoma, squamous cell carcinoma and adenocarcinoma, constitutes >80% of all lung cancer cases (3). The 5-year overall survival rate of NSCLC is poor despite great advances being made in diagnosis and treatment (4). Although cigarette smoking is the major risk factor for lung cancer, numerous genes have been reported to participate in lung carcinogenesis (5-7).

Semaphorin family proteins, which contain a conserved N-terminal Sema domain of 400-500 amino acids (8), comprise 8 classes with membrane-anchored and cleaved extracellular domain forms (9). The cleaved extracellular domain, such as SEMA3E (10), is modified from the

membrane-anchored forms by proteolytic effects (11,12). This proteolytic process is executed by the A disintegrin and metalloprotease (ADAM) family. For example, SEMA3C can be cleaved by ADAMTS1 (13) and SEMA5B can be cleaved by ADAM17 (14).

Initially, the semaphorin family proteins were discovered to regulate axon growth and neuronal migration (15,16). Recently, several studies have found that semaphorins are involved in cardiac/skeletal development (17), the immune response (18), the regulation of angiogenesis (19) and tumor growth, as well as metastasis (20). Class 3 semaphorins, such as SEMA3B and SEMA3F have been reported to be regulated by DNA methylation (21,22) and are related to various carcinogenic processes in the lungs, for example angiogenesis and metastasis (15,23-25) and tumor suppressor activities (26-28). However, whether other classes of the semaphorin family are subject to methylation regulation or are involved in carcinogenic processes in the lungs remains unclear.

Previously, a comprehensive analysis of the gene expression signature performed by the authors in non-smoking women with lung adenocarcinoma revealed that the downregulation of *SEMA5A* was associated with a poor overall survival (29). SEMA5A belonging to class V of the semaphorin family, is an integral membrane protein containing the Sema domain, 7 thrombospondin type-1 repeats and a short cytoplasmic domain (23,30). SEMA5A has been reported to have both a membrane-bound (8,31) and cleaved extracellular domain (32). Sheddases, which are the members of the ADAM protein families, are known to be majorly involved in ectodomain shedding by cleaving the extracellular portions of transmembrane proteins (33). However, the role of sheddase responsible for releasing the ectodomain from membrane-bound SEMA5A has yet to be identified.

In addition, as regards the function of *SEMA5A*, it was implicated as a susceptible gene related to Cri-du-chat syndrome (34) and autism (35). SEMA5A has also been reported to promote angiogenesis by increasing endothelial cell proliferation and decreasing apoptosis (36), and to have high tumorigenic and metastatic potential in pancreatic and gastric tumors (37-39). On the other hand, some studies have demonstrated that SEMA5A also plays the role of a tumor suppressor. For instance, SEMA5A maintains the epithelial phenotype of malignant pancreatic cancer cells (40), and inhibits glioma cell motility through the RhoGDIα-mediated inactivation of RAC1 GTPase (41) and the actin cytoskeleton (42). However, little is known about the mechanisms and functional role of the downregulation of *SEMA5A* in lung adenocarcinoma cells. Therefore, this study aimed to elucidate the mechanisms associated with low endogenous expression levels of *SEMA5A* in lung adenocarcinoma and to determine functional roles in lung carcinogenesis.

Materials and methods

Cells and cell culture. Cancerous lung cell lines (CL1-0, CL1-5, A549, and H1299) (gifts from Dr Pan-Chyr Yang) and normal cells (BEAS-2B) (a gift from Dr Pan-Chyr Yang) were cultured in RPMI-1640 medium (Gibco; Thermo Fisher Scientific) with 1% streptomycin/puromycin (Biological Industries) and 10% fetal bovine serum (FBS; Biological Industries). Brain metastatic lung adenocarcinoma Bm7 cells (generated in the authors' laboratory) were cultured in DME/F12 plus 10% FBS (43). The cultured plates were maintained at 37˚C in a humidified atmosphere with 5% CO_2. Another normal lung cell line (MRC-5) and human bronchial epidermal cells (16HBE) (a gift from Dr. Kuo-Ting Chang) were grown in Eagle's Minimum Essential Medium (Gibco; Thermo Fisher Scientific) under the same conditions.

Cell line authentication. Cell experiments were performed on cells that were passaged <20 times, and were routinely tested for mycoplasma using the PCR Mycoplasma Detection kit (ABM Inc., Vancouver, Canada). The identity of the cell lines was authenticated by short-tandem repeat (STR) analysis (Mission Biotech Inc., Taipei, Taiwan) in February, 2018.

Endogenous expression of SEMA5A. To quantify the transcriptional expression of *SEMA5A* in different cellular models, total RNA was isolated using TRIzol reagent (Ambion) and purified by precipitation with isopropanol (Sigma-Aldrich). A NanoDrop™ 2000 spectrophotometer (Thermo Fisher Scientific) was used to assess the purity and quantity of the RNA. A high Capacity cDNA Reverse Transcription kit (Thermo Fisher Scientific) was used to synthesize the cDNA from 1 μg of total RNA of each cell line. The final cDNA products were used as the templates for expression analysis using quantitative PCR (qPCR).

qPCR. The quality and quantity of the RNA were measured using a NanoDrop™ 2000 spectrophotometer (Thermo Fisher Scientific). A total of 1 μg of total RNA from each cell line was reverse transcribed using the High Capacity cDNA Reverse Transcription kit (Thermo Fisher Scientific). The reaction was carried using thermal cycling conditions, including annealing at 25˚C for 5 min, an extension temperature at 42˚C for 1 h and inactivation temperature at 70˚C for 15 min. The final cDNA products were used as the templates for subsequent qPCR with the following thermal cycling conditions. Denaturation temperature at 95˚C for 15 sec, anneal/extend temperature: 60˚C for 1 min for 40 cycles. RT-qPCR was performed using SYBR-Green (Roche) on an ABI 7900 system (Life Technologies; Thermo Fisher Scientific) according to standard protocols. All individual experiments were carried out in triplicate. Relative quantification, ΔΔCq (cycle threshold) (44), was applied using glyceraldehyde 3-phosphate dehydrogenase (*GAPDH*) as an internal control and empty group as a reference control.

Impact of methylation on gene expression. As a number of tumor suppressor genes are inactivated via hypermethylation within the promoter region (45,46), this study examined the role of methylation in regulating the expression of *SEMA5A*. The A549, H1299 and BEAS-2B cells were seeded on a 6-well plate, and after 24 h, the cells were treated with 5 or 10 μM of 5-aza-2'-deoxycytidine (5-aza; Sigma-Aldrich). The quantification of the expression levels was carried after 3 days of treatment.

To quantify the methylation levels of multiple CpG sites in the 5'untranslated region of *SEMA5A*, bisulfite treatment was first performed with an EpiTect Fast bisulfite conversion

kit (Qiagen) according to the manufacturer's instructions, and a pre-designed PyroMark CpG assay (Hs_*SEMA5A*_03_PM PyroMark CpG assay, PM00021203, Qiagen) was used. Specific CpG sites, including Chr5: 9545395, 9545400, 9545407, 9545409 and 9545417 were examined.

Overexpression of SEMA5A in lung adenocarcinoma cells. Full-length *SEMA5A* cDNA (3,225 bp) tagged with a Flag epitope was inserted into a pZeoSV2$^+$ viral expression vector with the *Not*I and *Asi*SI restriction enzymes (Addgene). The pZeoSV2$^+$-*SEMA5A*-Flag plasmid was transiently transfected into the A549 and H1299 cell lines using TransIT-2020 transfection reagent (MirusBio) according to the manufacturer's instructions. The empty pZeoSV2$^+$ viral expression vector was used as a control. All sequences were verified by Sanger sequencing (First Core Laboratory, College of Medicine, National Taiwan University). mRNA levels were quantified by RT-qPCR using *SEMA5A*-specific primers (forward, 5'-GTC TATACTTACTGCCAGCG-3' and reverse, 5'-GTTAAA TGCCTTGATGGCCTC-3') and *GAPDH*-specific primers (forward, 5'-TGCACCACCAACTGCTTAG-3' and reverse, 5'-GATGCAGGGATGATGTTC-3'). Protein levels were examined by western blot analysis.

Cleavage of SEMA5A by ADAM17. To examine the proteolytic effects of ADAM17 on SEMA5A, the H1299 cells were transfected with *SEMA5A* overexpression plasmid and treated with active recombinant ADAM17 (BioVision). The amount of administering ADAM17 was 0.66 μg for 6-cm dish. Cell lysates and media were collected at 2 days following transfection. Bovine serum albumin (BSA) was added externally to the culture media as the spike-in control, and all proteins in the medium were concentrated using a 10K Acrodisc syringe filter (Pall Life Sciences).

Western blot analysis. Total cell lysates of A549 and H1299 cells transfected with pZeoSV2$^+$-*SEMA5A*-Flag plasmid or empty vector were prepared. Proteins (30 μg) were separated by 10% sodium dodecyl sulfate-polyacrylamide gel electrophoresis (SDS-PAGE), and then electrotransferred onto polyvinylidene difluoride (PVDF) membranes (Bio-Rad Laboratories). After blocking with 5% milk, the membranes were incubated with anti-SEMA5A (1:1,000, Cat. no. PA5-26066, Thermo Fisher Scientific), anti-GAPDH antibody (1:20,000, Cat. no. GTX100118, GeneTex), or anti-BSA antibody (1:5,000, Cat. no. GTX79812, GeneTex). Following incubation overnight at 4˚C, the membranes were then incubated with horseradish peroxidase-conjugated anti-IgG (1:5,000, Cat. no. GTX213110, GeneTex) at room temperature for 1 h, and the blots were developed with the chemiluminescent western blotting reagent (Millipore). Western blot images were further analyzed using Gel-Pro Analyzer v6.3 software (Meyer Instruments) to obtain the optical density values of SEMA5A and GAPDH antibodies.

Isolation and amplification of total RNA for gene expression profiling. The mRNA detection and analysis were performed as previously described (47). Briefly, the cDNA was synthesized from total RNA primed with T7 Oligo(dT) and amplified using an Illumina TotalPre RNA Amplification kit (Ambion). The second strand of cDNA was synthesized by employing DNA polymerase and RNAase H to simultaneously degrade the RNA and synthesize the second strand of cDNA. Following cleanup, *in vitro* transcription was conducted to synthesize biotinylated complementary RNA (cRNA). Following amplification, the cRNA was hybridized to Illumina Human HT-12 v4 BeadChips (Illumina) for 16 h. Following hybridization, the BeadChip was washed and stained with streptavidin-Cy3 dye. The intensity of the beads' fluorescence was detected by HiScan SQ (Illumina), and the results were analyzed using BeadStudio v2011.1 software.

After scanning, the intensity data of Illumina BeadChips were analyzed using Partek v7.0 software (Partek). Background-adjusted signals were normalized by a quantile normalization algorithm. Student's t-tests and Bonferroni P-value adjustment were utilized to identify differentially expressed genes. Principle component analysis (PCA) was utilized to evaluate the similarity of the gene expression profiles. Hierarchical clustering analysis and the Genesis program were used to generate visual representation of expression profiles. All data have been deposited at the Gene Expression Omnibus (GEO, GSE114578). Furthermore, ingenuity pathway analysis (Ingenuity Systems Inc.) was applied to comprehend the biological functions and signaling pathways of differentially expressed genes.

Analysis of cell proliferation. A total of 3,000 lung adenocarcinoma cells (A549 & H1299) were seeded in 96-well plates in triplicate and incubated for 12 h at 37˚C in a CO_2 incubator. The day after seeding, the cells were transfected with pZeoSV2$^+$-*SEMA5A*-Flag plasmid or empty vectors. Following transfection, the cells proliferative activity was measured by 3-(4,5-dimethylthiazol-2-yl)-2,5-diphenyltetrazolium bromide (MTT) (EMD Biosciences) assay at 24, 48 and 72 h, respectively. The absorbance of the A549 and H1299 cells was then measured using a microtiter plate reader (BioTek) at 570 nm.

Immunohistochemistry. The A549 (3,000 cells) or H1299 (3,000 cells) cells were seeded on silane coated micro slides (Muto pure chemicals Co.) with the same cell density and transfection concentration as MTT assay. The cells were fixed with 4% paraformaldehyde (Sigma-Aldrich) at 48 h following transfection. The cell membrane was damaged by 0.1% Triton X-100 (Mallinckrodt Specialty Chemicals Co) and blocked with 2% bovine serum albumin (Sigma-Aldrich). Ki-67 primary antibody (1:400, #9129, Cell Signaling Technology) and anti-rabbit IgG secondary antibody (1:800, #8889, Cell Signaling Technology) were used for Ki-67 detection at a wavelength of 550/580 nm. The incubation conditions for the primary antibody were 4˚C overnight, and for the secondary antibody they were 2 h at room temperature. Cell nuclei were stained with Hoechst 33342 (#B2261, 1 μg/ml, Sigma-Aldrich) and detected at wavelength of 360/460 nm. The incubation conditions for Hoechst 33342 were 30 min at room temperature. Images were acquired using the Zeiss AxioImager A1 system (Carl Zeiss).

Clonogenic assay. The A549 (300 cells), H1299 (300 cells) and Bm7 (300 cells) cells were first seeded in 6-well plates for 24 h, and transfected with pZeoSV2$^+$-*SEMA5A*-Flag plasmid or empty vectors. After 2 weeks, the cells were fixed using

3:1 methanol-acetic acid and stained using 0.1% crystal violet (Sigma-Aldrich) for 10 min at room temperature. Finally, the stained plates were dried and used for image acquisition using microscopic (x100 magnification) evaluation. Colonies containing >50 cells under a stereomicroscope were counted.

Gap closure assay. Following 24 h of transfection, $2x10^4$ cells of A549 and H1299 were seeded into 24-well plates with a sterile culture insert and grown to ~90% confluence in RPMI-1640 medium containing 10% FBS and changed to 2% FBS when removing the cassettes. The culture inserts were removed and an image of the gap at 0 h was captured. The cells were further incubated at 37˚C in a CO_2 incubator for 36 h, and images were captured at 24 and 36 h to measure the progress of gap closure.

Cell migration. Migration assays were carried out using a 24-well Transwell unit (Corning, Inc.). The upper chamber of the Transwell unit was loaded with $4x10^4$ cells/well in 0.2 ml serum-free RPMI-1640 medium, and the lower chambers were loaded with 0.6 ml RPMI-1640 containing 10% FBS as a chemoattractant. The A549 and H1299 cells were then incubated for 24 h at 37˚C. A methanol-acetic acid (3:1) mixture was then added to the lower chamber to fix the cells for 20 min at room temperature followed by staining with 0.1% crystal violet for a further 20 min at room temperature. Cells on the upper side of the membrane surface were removed by scraping with a cotton swab, and the cells that passed through the filter were de-stained using 10% acetic acid. The absorbance was measured at 570 nm with an enzyme-linked immunosorbent assay (ELISA) reader (BioTek Instruments). Cells transfected with empty vector were used as the controls.

Time-lapse migration assay. The experiment was performed as previously described (43). Briefly, cells were cultured on dishes coated with collagen (10 μg/ml) overnight and then cultured in serum-free conditioned medium. Cell movement was detected under A-Plan objectives (X5; 0.55 NA) using an inverted microscope (Axio Observer Z1, Zeiss) in 37˚C chambers. Images were collected from CCD video cameras (AxioCam MRm, Zeiss) at 20-min intervals for a total of 16 h using MetaMorph software (Molecular Devices Corp.). The accumulated distance was measured by tracking each cell nuclei for 30 individual cancer cells in each group using the Track Point function of NIH ImageJ v1.43 software.

Lung cancer animal model. The *SEMA5A*-Flag plasmid was transiently transfected into Bm7 lung cancer cells with stable luciferase expression. The following day, the Bm7 cells ($2x10^6$ cells in 50 μl of PBS) were mixed with 50 μl of Matrigel and then implanted into 6-8 week-old male SCID mice (weighing 20-25 g; BioLASCO) by the subcutaneous route at two separate sites (right and left side) of the back (each group had 4 mice; 2 groups). Mice were housed in specific pathogen-free rooms with one group in one cage at room temperature (20-23˚C), 40-60% relative humidity and under a 12-h light-dark cycle, with free access to food and water. No cachexia and ascites in mice were observed in this study. As Bm7 lung tumors had luciferase, the tumor volume was detected using an IVIS Spectrum Imaging system (Xenogen). Prior to image acquisition, the mice were subsequently administered D-luciferin via intraperitoneal injection and photons emitted from the mice were detected using an imaging system. Tumor size and distribution *in vivo* were quantified as photons/second. The maximum length and width exhibited by a single subcutaneous tumor in this study did not exceed 1.5 cm. The maximum tumor volume calculated by signal was 500 mm^3 using the formula, (length x $width^2$)/2. Anesthesia was induced and maintained with 2.5% isoflurane (Panion & BF Biotech Inc.) in 100% oxygen in an anesthetic chamber when mice were monitored by an IVIS Spectrum Imaging system. The mice were sacrificed by using carbon dioxide (CO_2) at a displacement rate from 10 to 30% of the chamber volume per minute for mouse euthanasia and death was verified by physical methods following euthanasia on day 21, including no heartbeat, no pupillary response to light and no respiratory pattern.

This animal model followed protocols approved by the Institutional Animal Care and Use Committee of China Medical University and Hospital (animal protocol no. 2016-102). Suitable humane endpoints were included in the approved animal experiments. In this study, the mouse experiment was terminated by euthanasia (using carbon dioxide) on day 21 or animals that reached humane endpoints when the tumor size was near 1,000 mm^3 or unexpected circumstances, such as illnesses (infection, difficulty breathing, etc.) and injuries (necrosis or bleeding in tumors). The mice were sacrificed by using carbon dioxide (CO_2) at a displacement rate from 10 to 30% of the chamber volume per minute for mouse euthanasia and death was verified by methods, including no heartbeat, no pupillary response to light, and no respiratory pattern for at least 5 min.

Kaplan-Meier survival analysis. Kaplan-Meier survival analyses were conducted using Kaplan-Meier Plotter for lung cancer (48,49), an online platform (http://www.kmplot.com/lung), using *SEMA5A* probe (Affy ID: 229427_at) and adenocarcinoma in histology restriction. In total, Kaplan-Meier Plotter analyzed 1,715 patients for survival analysis, which included 1,120 patients in 7 GEO datasets (GSE4573, GSE14814, GSE8894, GSE19188, GSE3141, GSE31210, GSE29013 and GSE37745), 462 patients in the caArray, and 133 patients in The Cancer Genome Atlas (TCGA). The log rank test was used to determine differences in the survival rate between the high and low expression groups.

Statistical analysis. Data are expressed as the means ± standard deviation (SD) of at least 3 independent experiments. Student's t-tests and Bonferroni P-value adjustment were utilized to identify differentially expressed genes. P-values <0.05 were considered to indicate statistically significant differences.

Results

Association of SEMA5A expression in lung cancer tissues with a poor overall survival. In previous genomic studies, it was found that the downregulation of *SEMA5A* in non-smoking women with lung adenocarcinoma was associated with a poor overall survival (29,50,51). To validate this phenomenon in a Caucasian population, another publicly available dataset

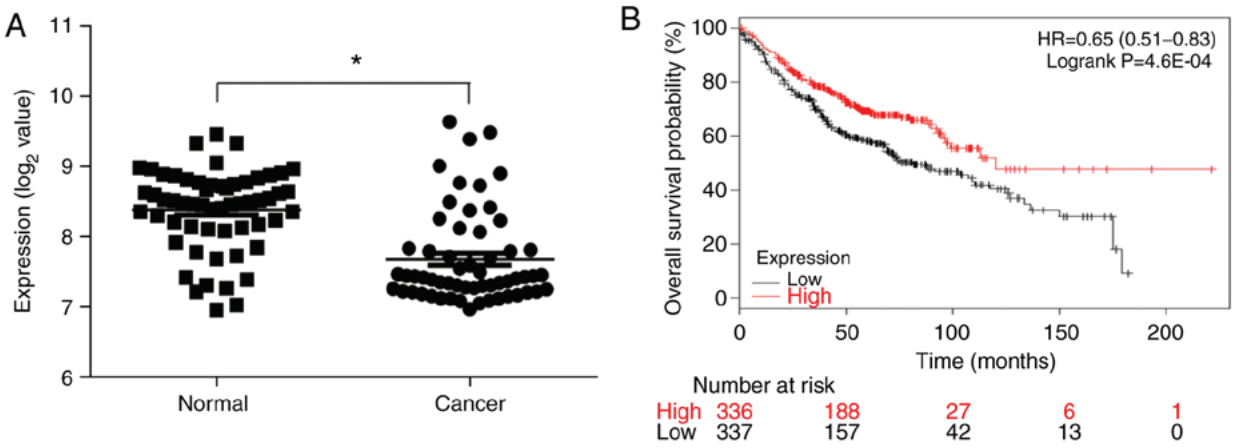

Figure 1. Downregulation of *SEMA5A* in lung adenocarcinoma tissues is associated with poor overall survival. (A) Expression levels of *SEMA5A* were examined in normal and lung adenocarcinoma (cancer) tissues from the study by Selamat *et al* (52); *P<0.01. (B) Survival analysis was performed based on the expression levels of *SEMA5A* using a Kaplan-Meier plotter (www.kmplot.com/lung) (48,49). Patients were divided into the high and low expression groups based on the median value of all samples (n=1,715). P-values were calculated using a log-rank test. HR, hazard ratio; *SEMA5A*, semaphorin 5A.

was examined (52). As shown in Fig. 1A, *SEMA5A* was also significantly (P<0.01) downregulated in cancer tissues as compared to adjacent normal control tissues. Furthermore, the survival of lung adenocarcinoma patients in the new dataset for >15 years was examined using Kaplan-Meier plotter (www.kmplot.com/lung) (49). In total, 1,715 patients were used for survival analysis, which included 1,120 patients in 7 GEO datasets (GSE4573, GSE14814, GSE8894, GSE19188, GSE3141, GSE31210, GSE29013 and GSE37745), 462 patients in the caArray, and 133 patients in The Cancer Genome Atlas (TCGA). Patients were divided into the high and low expression groups based on the median expression value of *SEMA5A*. The results of Kaplan-Meier survival analysis revealed that the lung adenocarcinoma patients with higher expression levels of *SEMA5A* had a lower risk of death (hazard ratio, 0.65), i.e., a higher overall survival probability (Fig. 1B), indicating the potential utility of *SEMA5A* as a prognostic marker for patients with lung adenocarcinoma.

Mechanisms responsible for the lower SEMA5A expression in lung adenocarcinoma cells. Since *SEMA5A* was downregulated in non-smoking female lung adenocarcinoma patients (29), the endogenous expression levels of *SEMA5A* were then examined in 4 lung adenocarcinoma cell lines (CL1-5, CL1-0, A549 and H1299), 2 normal lung cell lines (MRC-5 and BEAS-2B) and human bronchial epithelial cells (16HBE). The results of RT-qPCR revealed that *SEMA5A* was significantly (P<0.01) downregulated in all lung adenocarcinoma cell lines (Fig. 2A). The results of western blot showed that the endogenous SEMA5A proteins in lung adenocarcinoma cell lines were lower than that of BEAS-2B (Fig. 2B); however, it was not downregulated the 2 other normal control cell lines (MRC-5 and 16HBE). Therefore, the A549, H1299 and BEAS-2B cells were arbitrarily selected for use in the following experiments.

Subsequently, to investigate the mechanisms leading to a lower *SEMA5A* expression in lung adenocarcinoma cells, we first examined the role of methylation in regulating endogenous expression by treating the A549, H1299 and BEAS-2B cell lines with 5-aza. The expression levels of *SEMA5A* were significantly (P<0.01) increased in a dose-dependent manner in the A549 and H1299 lung adenocarcinoma cell lines, whereas they were not altered in the BEAS-2B normal cells (Fig. 2C). Moreover, pyrosequencing analysis was performed to identify the specific CpG sites of methylation in *SEMA5A*. In total, 5 CpG sites in the 5'untranslated region of *SEMA5A* were examined (Fig. 2D top panel). The 4 CpG sites in the A549 cells and 3 CpG sites in the H1299 cells revealed a significantly higher methylation percentage as compared to the normal BEAS-2B cells (Fig. 2D bottom panel), indicating that methylation plays a role in regulating the expression of *SEMA5A* in lung adenocarcinoma cells.

Subsequently, *SEMA5A* was transiently overexpressed in the A549 and H1299 cells. As shown in Fig. 3A, the mRNA levels of *SEMA5A* in the A549 and H1299 cells following transfection were significantly (P<0.01) increased. Western blot analysis also validated that the SEMA5A protein levels increased in both the A549 and H1299 cells upon transfection with *SEMA5A* expression plasmid (Fig. 3B). Since a previous study demonstrated that the mature form of SEMA5B was proteolytically processed by ADAM17 (14), this study also examined whether SEMA5A can be cleaved by ADAM17. H1299 cells overexpressing *SEMA5A* were treated with active recombinant ADAM17. As shown in Fig. 3C and D, the amount of SEMA5A in the cell lysate from the A549 (Fig. 3C) and H1299 (Fig. 3D) cells was lower in the presence of ADAM17. By contrast, the amount of SEMA5A in the medium increased (Fig. 3C and D), suggesting that membrane-bound SEMA5A was released into the medium in the presence of ADAM17.

Identification and function of SEMA5A-regulated genes using microarray. In order to investigate the functional role of *SEMA5A*, the functions of *SEMA5A*-regulated genes were first investigated. Total RNA was extracted 24 h following the transfection of *SEMA5A* plasmid into the A549 cells. Differentially expressed genes regulated by *SEMA5A* were identified by Illumina Human HT-12 v4 Bead Chips. The criteria for the selection of differentially expressed genes consisted of a fold change ≥3 and significant differences (P<0.05). In total, 350 differentially expressed probes were

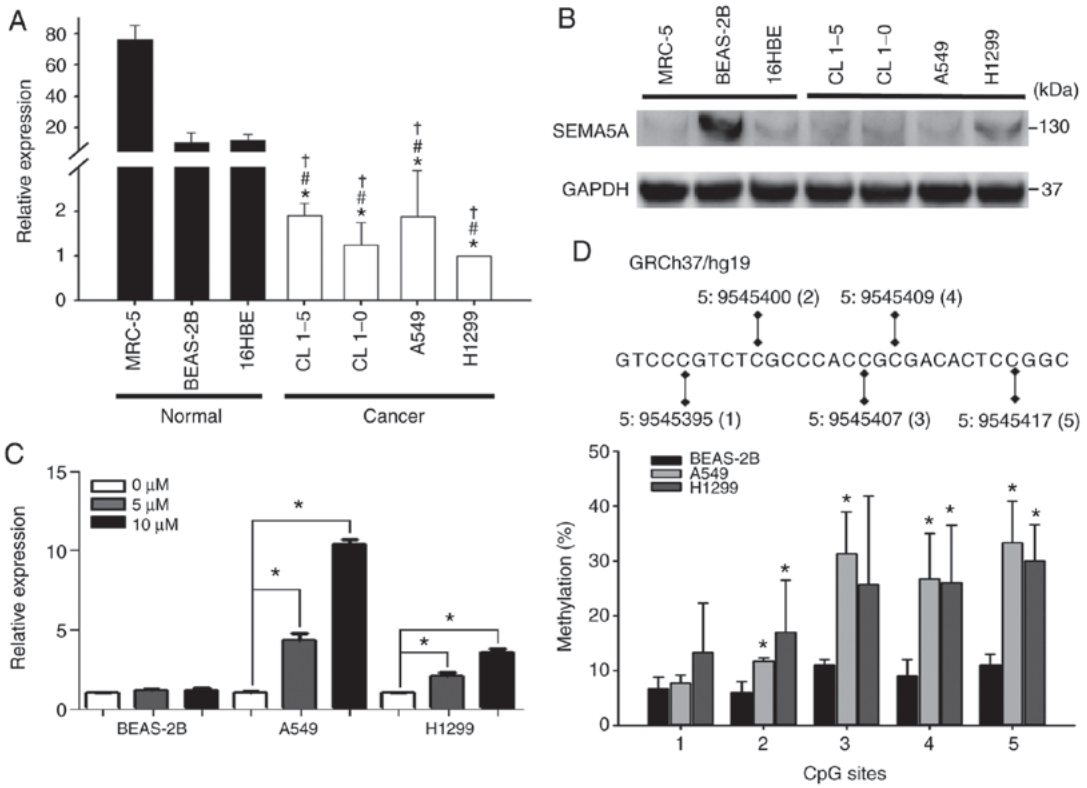

Figure 2. Lower expression levels and hypermethylation of *SEMA5A* observed in lung adenocarcinoma cells. (A) Endogenous expression levels of *SEMA5A* in lung adenocarcinoma cells. Total mRNA was extracted from lung adenocarcinoma cells (CL1-5, CL1-0, A549 and H1299) and normal controls (MRC-5, BEAS-2B and 16HBE). The endogenous expression levels of *SEMA5A* were measured by RT-qPCR. *GAPDH* was used as a loading control. Bars represent the means ± SD of 3 independent experiments; *P<0.01 as compared to MRC-5 cells; #P<0.01 as compared to BEAS-2B cells; †P<0.01 as compared to 16HBE cells. (B) Western blot analysis of endogenous expression levels of *SEMA5A* in lung adenocarcinoma cells and normal controls. GAPDH was used as an internal control. (C) Relative expression of *SEMA5A* mRNA in cells treated with 5 and 10 μM of the methylation inhibitor, 5-aza-2-deoxycytidine (5-aza), for 3 days. Relative expression levels of *SEMA5A* were normalized against the untreated group of each cell line. (D) Methylation levels of *SEMA5A*. Upper panel, scheme of CpG sites in the 5'-untranslated region of *SEMA5A* for pyrosequencing. CpG sites were numbered as shown in parentheses according to genome assembly version GRCh37/hg19. Lower panel, quantification of DNA methylation of *SEMA5A*. Genomic DNA was extracted from the A549, H1299 and BEAS-2B cells and treated with bisulfide to examine the methylation percentage of CpG sites by pyrosequencing; *P≤0.05 as compared to BEAS-2B cells. *SEMA5A*, semaphorin 5A.

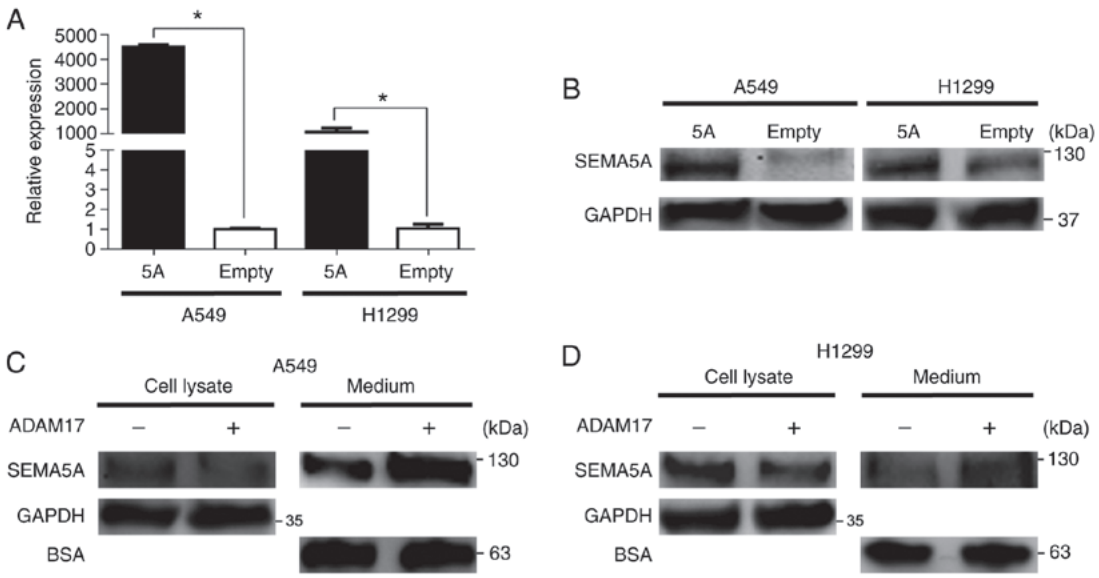

Figure 3. SEMA5A is cleaved by ADAM17. (A) Relative expression levels of *SEMA5A* in A549 and H1299 cells overexpressing *SEMA5A* were measured by RT-qPCR. *GAPDH* was used as a loading control. Bars represent the means ± SD of 3 independent experiments. *P<0.01 as compared to the empty control vector. (B) Western blot analysis of SEMA5A in A549 and H1299 cells overexpressing *SEMA5A*. GAPDH was used as an internal control. (C and D) Western blot analysis of SEMA5A in the cell lysate and the medium following treatment with ADAM17. (C) A549 and (D) H1299 cells were transfected with *SEMA5A* and treated with active recombinant ADAM17 (0.66 μg/6-cm dish). GAPDH was used as an internal control. Bovine serum albumin (BSA) was used as the spike-in control. SEMA5A, semaphorin 5A; ADAM17, A disintegrin and metalloprotease 17.

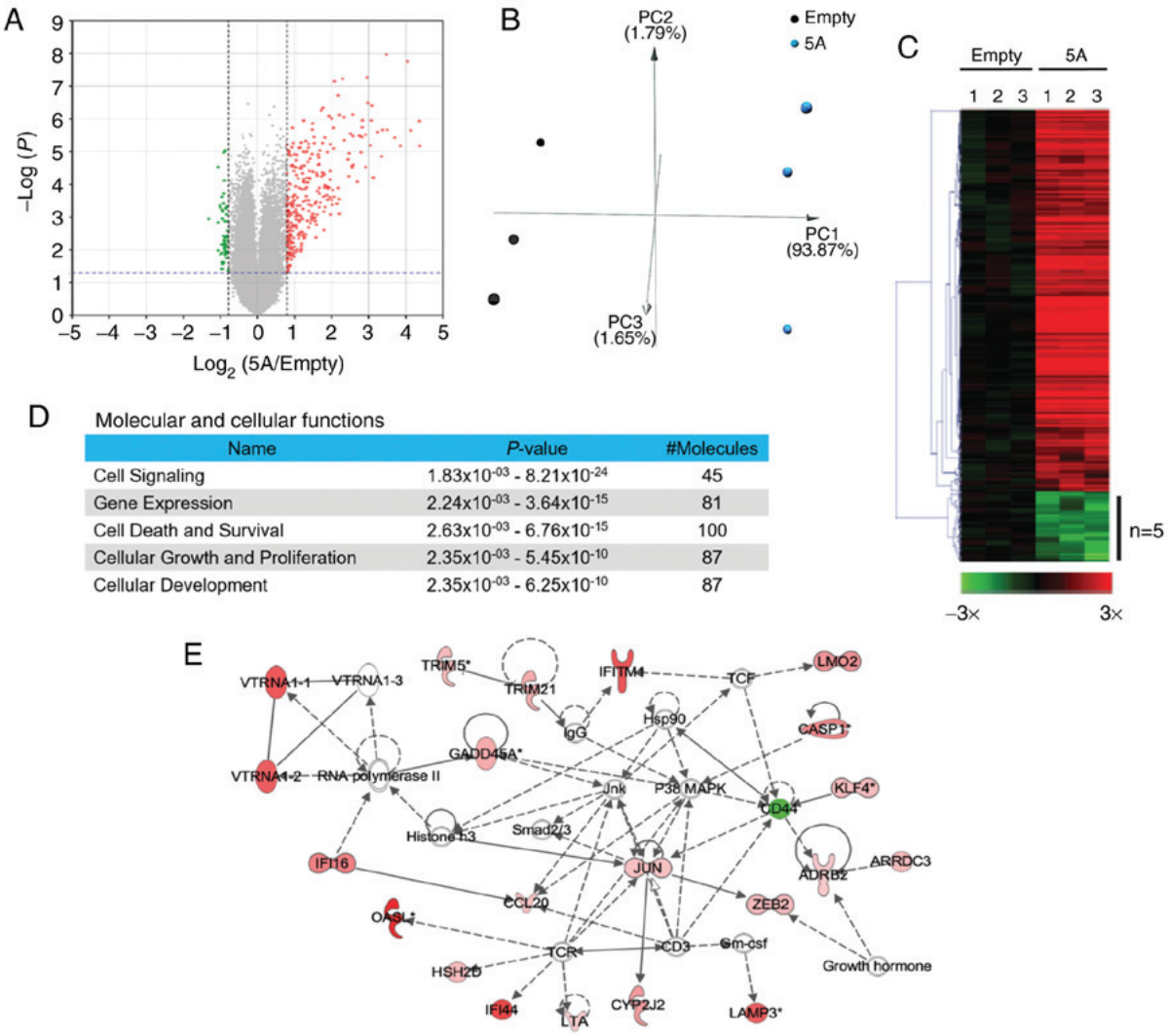

Figure 4. Functions of *SEMA5A*-regulated genes are involved in cellular growth and proliferation in lung adenocarcinoma cells. (A) Volcano plots of differentially expressed genes. Total RNA was extracted 24 h following transfection and genomic profiling was examined by Illumina Human HT-12 v4 Bead Chips. The criteria for the selection of *SEMA5A*-regulated genes were a fold change ≥3 and P<0.05. Red points, upregulated genes in cells overexpressing *SEMA5A*; green points, downregulated genes; gray points, genes without significant changes. (B) Principal component analysis (PCA) of A549 cells overexpressing *SEMA5A*. PCA was plotted using the expression of differentially expressed probes following quantile normalization. Each dot represents each sample. (C) Heatmap and hierarchical cluster analysis of *SEMA5A*-regulated genes. The rows represent genes, and the columns represent samples. Red, upregulated genes in cells overexpressing *SEMA5A*; green, downregulated genes; black, unaltered expression as compared to the empty control. (D) Molecular and cellular functions of *SEMA5A*-regulated genes using ingenuity pathway analysis. (E) Network of *SEMA5A*-regulated genes involved in cellular movement, cellular growth and proliferation. The solid lines indicate direct evidence of an interaction between the 2 genes according to published literature reports, whereas the dashed lines indicate indirect interactions between molecules as supported by information in the Ingenuity knowledge base. Red areas denote genes that were upregulated in cells overexpressing *SEMA5A* and green areas indicate downregulated genes. SEMA5A, semaphorin 5A.

identified. The volcano plot illustrated in Fig. 4A represents 350 differentially expressed probes (a.k.a. genes), with 296 probes upregulated (red points) and 54 ones downregulated (green points) (Fig. 4A and Table SI). Genes that did not meet the criteria of differentially expressed genes were shown in gray (Fig. 4A). Principal component analysis, a visualization tool to used illustrate that the expressional profiling of the 350 differentially expressed probes between the *SEMA5A* group and control group, indicated that the distribution between samples overexpressing *SEMA5A* (cyan spots) and the controls (black spots) was separated, indicating different expressional profiling of the selected genes between the *SEMA5A* group and the control group (Fig. 4B).

A heatmap with hierarchical clustering, a common method of visualizing the relative intensity of gene expression by arranging genes together based on the similarity of their expressional levels, is presented in Fig. 4C. The relative intensities of the 296 upregulated probes are shown in red, and those of the 54 downregulated ones are shown in green.

Furthermore, network analyses were performed by ingenuity pathway analysis. The dashed lines indicate indirect interactions between molecules as supported by information in the Ingenuity knowledge base. The results of pathway analysis revealed that these genes were involved in cell signaling, gene expression, cell death and survival, cellular growth and proliferation (Fig. 4D and Table SII). Network analysis also revealed the interactions among some of the differentially expressed genes. In one of the representative networks, although *SEMA5A* was not enriched in this network, contained genes which were involved in cellular movement, cellular

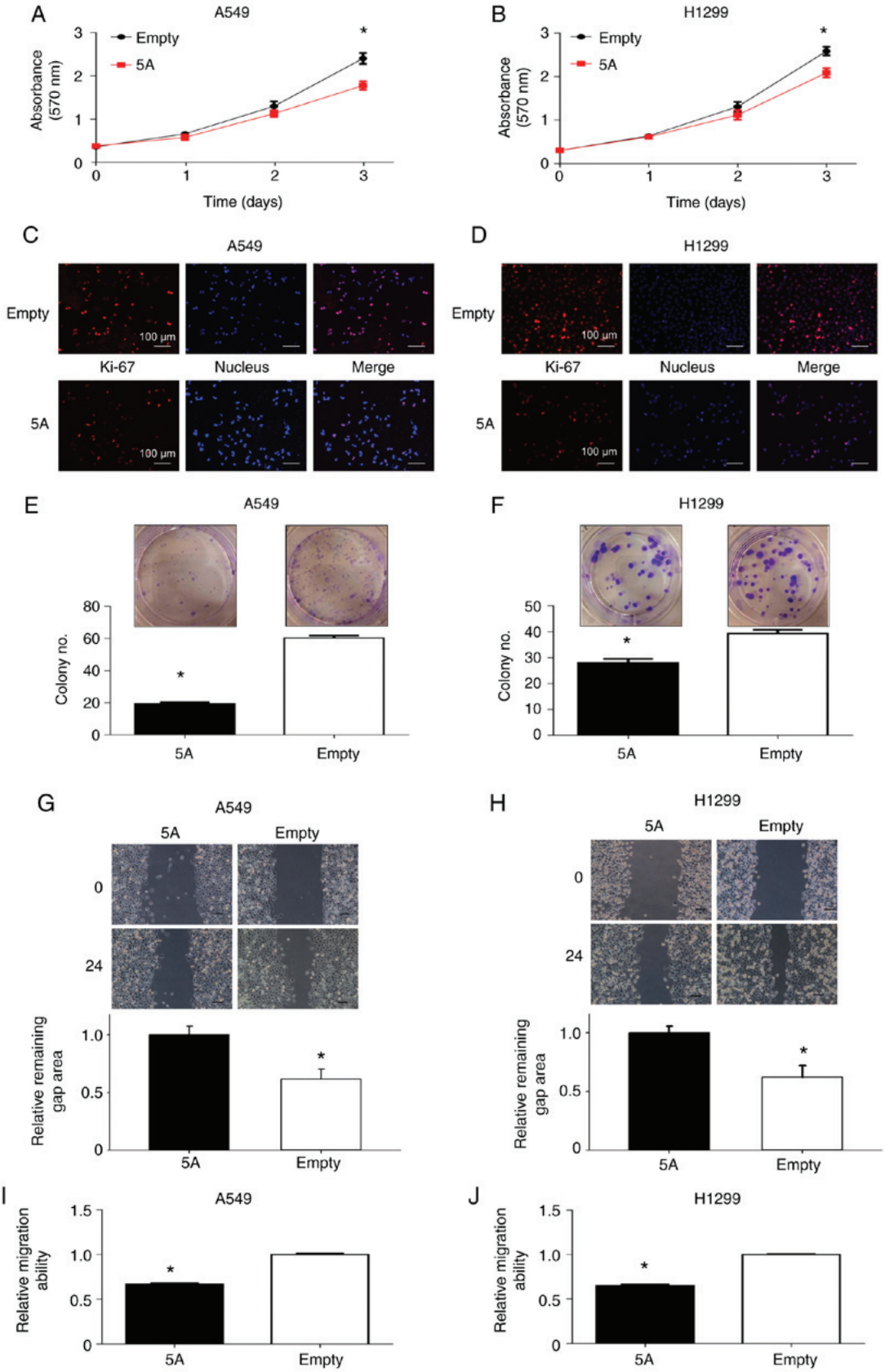

Figure 5. SEMA5A suppresses the proliferation and migration of lung adenocarcinoma cells. (A and B) MTT assays of (A) A549 and (B) H1299 cells overexpressing *SEMA5A* vs. empty vector. Proliferation assays were performed by the addition of MTT at different time points using 3,000 cells transfected with *SEMA5A* expression vector or empty control vector. The absorbance values indicate the proliferation status of the cells. (C and D) Immunohistochemistry assay of Ki-67 in (C) A549 and (D) H1299 cells overexpressing *SEMA5A*. Ki-67: A cellular marker for proliferation. Scale bar 100 μm. (E and F) Colony formation assays of (E) A549 and (F) H1299 cells overexpressing *SEMA5A*. (G and H) Representative pictures and quantification of gap closure assays of (G) A549 and (H) H1299 cells overexpressing *SEMA5A*. Images were acquired at 0 and 48 h. Scale bar, 100 μm. (I and J) Transwell migration assays of (I) A549 and (J) H1299 cells overexpressing *SEMA5A*. The absorbance values of migratory cells were normalized against the empty vector group. Bars represent the means ± SD of 3 independent experiments; *P<0.01 vs. empty vector. SEMA5A, semaphorin 5A.

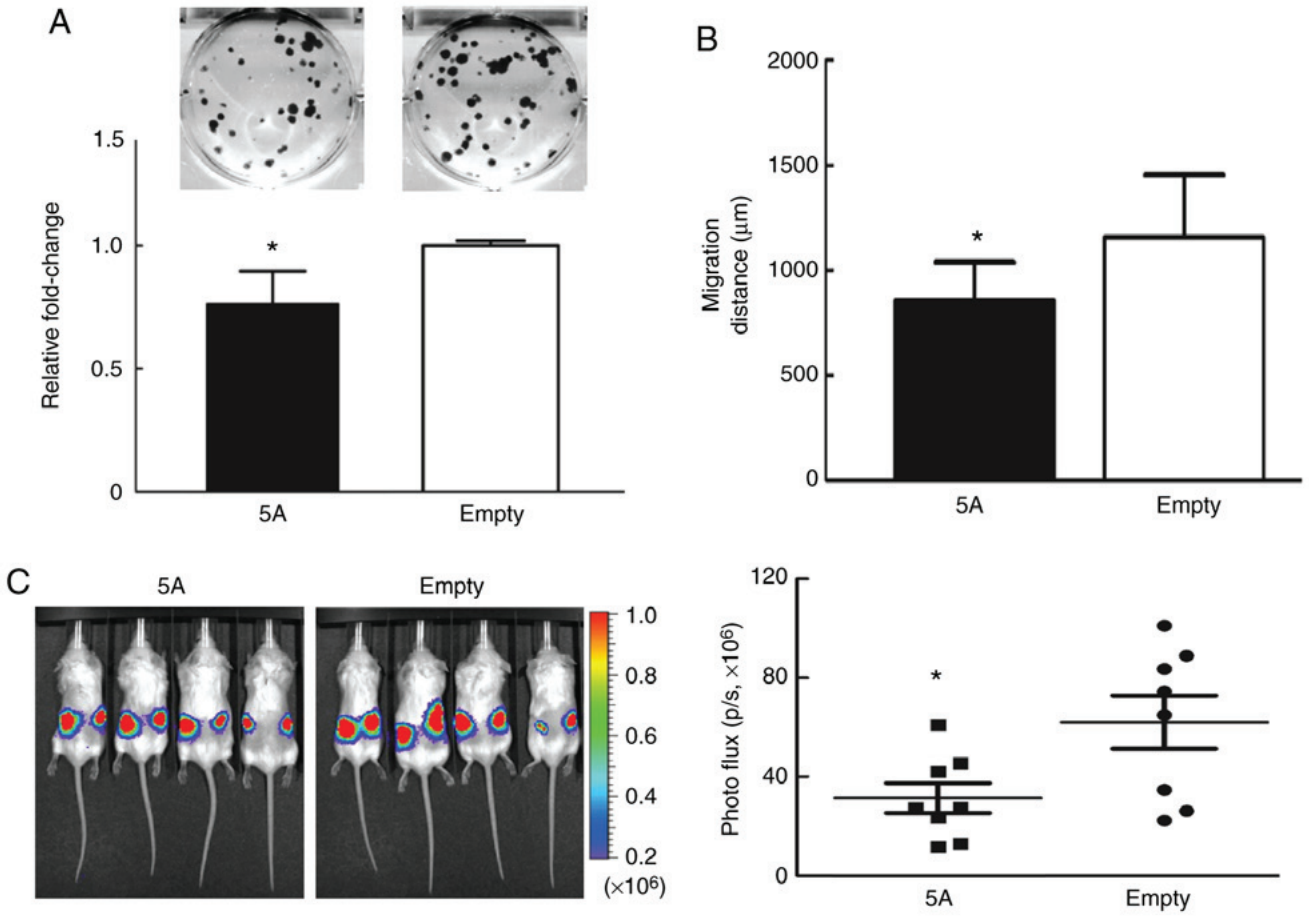

Figure 6. SEMA5A decreases tumor growth of Bm7 lung adenocarcinoma cells in SCID mice. (A) Colony formation assays of Bm7 cells overexpressing *SEMA5A*. (B) Migratory ability of *SEMA5A*-overexpressing Bm7 lung cancer cells using time-lapse video microscopy. Quantification of the migration distance over 16 h from 3 independent experiments. (C) Xenograft assays of Bm7 lung cancer cells on SCID mice. Bm7 cells overexpressing *SEMA5A* were injected subcutaneously into the backs of SCID mice and tumor images were examined using the IVIS Spectrum Imaging system. Left panel, quantitative signals from tumors on day 13; right panel, quantification of the intensity images. *P<0.01 vs. empty vector. SEMA5A, semaphorin 5A.

growth and proliferation, as shown in Fig. 4E, which was later validated by further functional analysis.

Functional roles of SEMA5A in lung adenocarcinoma. Based on the function of *SEMA5A*-regulated genes, the effects of SEMA5A on tumor growth by MTT assays were hence examined. The results revealed a significant decrement in the proliferation of both the A549 and H1299 cells overexpressing *SEMA5A* (Fig. 5A and B). In agreement with these results, immunohistochemistry assay of Ki-67, a cellular marker for proliferation, also revealed a markedly decreased amount of Ki-67 and cell numbers following transfection with the *SEMA5A* expression plasmid (Fig. 5C and D). Furthermore, *SEMA5A* overexpression reduced colony formation in both the A549 (Fig. 5E) and H1299 (Fig. 5F) cells. These results demonstrated the suppressive effects of SEMA5A on the proliferation and colony formation of lung adenocarcinoma cells.

Subsequently, the effects of SEMA5A on the mobility of lung adenocarcinoma cells were investigated by gap closure assay and Transwell migration assays. Both assays revealed that the overexpression of *SEMA5A* significantly suppressed the migratory abilities of both the A549 (Fig. 5G and I) and H1299 (Fig. 5H and J) cells. Previously, SEMA5A has been shown to impede the motility of human gliomas via the indirect inactivation of RAC1 and FSCN1 (41,42). However, the transcriptional levels of *RAC1* and *FSCN1* were not altered significantly in this study (Fig. S1).

Lastly, the role of SEMA5A in severe combined immunodeficiency (SCID) mice was examined. Since the growth of tumors in SCID mice using either A549 or H1299 lung cancer cells was not successful in pilot studies by the authors (data not shown), brain metastatic Bm7 lung cancer cells (43) were used to demonstrate the role of SEMA5A in *in vivo* experiments. Similar results were observed in the *in vitro* experiments (Fig. 6). *SEMA5A* overexpression reduced colony formation (Fig. 6A) and cell migration examined by time-lapse video microscopy (Fig. 6B). In the tumor xenograft assays, Bm7 cells overexpressing *SEMA5A* were injected subcutaneously into the backs of SCID mice to develop subcutaneous tumors. After 13 days, the tumor size was found to be significantly smaller in the *SEMA5A* group (Fig. 6C). No lymph nodes or distant organ metastases were detected during the experimental period.

Discussion

In a previous genomic study by the authors, *SEMA5A* was identified as a prognostic biomarker in non-smoking Taiwanese

women with lung adenocarcinoma (29). In this study, it was confirmed that the downregulation of *SEMA5A* in lung adenocarcinoma tissues was associated with a poor overall survival in different ethnic groups. In addition, lower levels of SEMA5A in lung adenocarcinoma cells were the result of both hypermethylation in the 5'untranslated region at the genetic level and cleavage to the secretory form. In addition, microarray analyses revealed that *SEMA5A*-regulated genes were involved in growth and proliferation. Finally, *in vitro* and *in vivo* analyses revealed the suppressive effects of *SEMA5A* overexpression on lung adenocarcinoma cell lines in terms of proliferation, colony formation and migration.

Semaphorins represent a large family of proteins, many of which are promising targets for interfering with cancer progression due to their roles in tumor angiogenesis, tumor growth and metastasis (27,53,54). In particular, previous studies have reported the roles of SEMA5A in the development of several types of cancer, such as pancreatic cancer, gastric cancer, ovarian cancer and gliomas (37,41,42,55,56). SEMA5A has been reported to enhance the invasion and metastasis of gastric cancer and pancreatic cancer cells (39,57) and has been shown to be associated with a poor survival in ovarian cancer (56). In contrast to this finding, a previous investigation by the authors revealed that the incidence of lung adenocarcinoma was associated with the downregulation of *SEMA5A* expression in non-smoking female lung adenocarcinoma patients, and that this down-regulation was associated with a poor overall survival (29). To investigate these seemingly opposing roles of SEMA5A in different types of cancer, this study first examined the endogenous expression levels of *SEMA5A* in lung adenocarcinoma cell lines. Consistent with the expression pattern in clinical tissues, the expression of *SEMA5A* was downregulated in lung adenocarcinoma cells as compared to their normal counterparts (Fig. 2A).

Furthermore, the inactivation of several tumor suppressor genes has been shown to be partly due to hypermethylation within the promoter region (45,46). Epigenetically disrupted gene expression can further alter various cancer-related processes, such as cell proliferation, apoptosis and angiogenesis (58,59). The abnormal DNA methylation of genes may be associated with clinical outcomes in lung cancer patients (60). This study found that hypermethylation in the upstream genetic loci was partly responsible for the downregulation of *SEMA5A* in lung adenocarcinoma cells, as has been previously reported for other tumor suppressor genes (45,46). In this study, when the cells were treated with the methylation inhibitor, 5-aza, the upregulation of *SEMA5A* was observed only in the cancer cell lines. Pyrosequencing results further identified the methylated CpG sites modulating the expression of *SEMA5A* in these cell lines, suggesting that aberrant methylation changes result in the inactivation of *SEMA5A* in lung adenocarcinoma cells (Fig. 2B and C). However, additional studies using larger numbers of tissue samples that contain clinical features are required to validate whether methylation changes of *SEMA5A* are involved in tumorigenesis.

Furthermore, this study demonstrated that SEMA5A can be possibly cleaved by ADAM17, which belongs to the protein family of disintegrins and metalloproteases (Fig. 3C and D). ADAM17 is involved in the release of a soluble ectodomain from membrane-bound pro-proteins. It has also been reported to be upregulated in non-small cell lung cancer (61), and this upregulation of ADAM17 can be caused due to ionizing radiation (62). Moreover, the silencing of *ADAM17* has been shown to suppress the migration and invasion of A549 cells *in vitro*, and tumor growth *in vivo* (63). Since previous studies have demonstrated that the mature form of SEMA5B is proteolytically processed by ADAM17 (14), and that the cleaved extracellular domain of SEMA5A decreases following the silencing *ADAM17* (32), this study assessed the proteolytic effect of recombinant ADAM17 on SEMA5A. The results suggested that the membrane-bound SEMA5A was exported to the medium following cleavage by ADAM17. However, further clarifications are required to conclude whether the endogenous ADAM17 in lung adenocarcinoma cells has enough proteolytic activity to shed membrane-bound SEMA5A.

The extracellular domain of SEMA5A is involved in angiogenesis (36). There is evidence to indicate an increase in proliferation and the upregulation of anti-apoptotic genes (e.g., *BCL-2* and *BIRC5)* following treatment of endothelial cells with the extracellular domain of recombinant SEMA5A (36). In addition, pancreatic cells transfected with the extracellular domain of SEMA5A exhibit a greater metastatic potential and an enhanced endothelial cell proliferative ability (64). These results suggest that the extracellular domain of SEMA5A plays a potential role in carcinogenesis.

However, this study found that the total amount of membrane-bound SEMA5A in lung adenocarcinoma cells was downregulated compared to normal lung cells. The transient overexpression of *SEMA5A* in lung adenocarcinoma cells had tumor-suppressive effects, such as decreasing cell proliferation, colony formation and migration (Figs. 5 and 6), although not increasing apoptosis (data not shown). Furthermore, lower expression levels of *SEMA5A* were found to be associated with a worse prognosis (Fig. 1B), which suggested the tumor suppressive role of SEMA5A in lung adenocarcinoma. Consistent with the findings of this study, lower endogenous SEMA5A levels have been found to be associated with increased invasiveness in glioma. Furthermore, SEMA5A has been shown to impede the motility of human gliomas upon its interaction with Plexin-B3 via the indirect inactivation of Rac1 through RhoGDIα, and the inactivation of protein kinase C (PKC) to phosphorylate fascin-1 (41,42). However, the transcriptional levels of *RAC1* and *FSCN1* did not alter significantly in this study (Fig. S1), and whether the levels and activity of these proteins are altered remains to be determined in lung adenocarcinoma cells.

On the contrary, a high expression of SEMA5A protein has been shown to be associated with poor overall survival outcomes in metastatic ovarian cancer (56) and to be associated with progression and metastasis in gastric cancer and pancreatic cancer (39,57). In explaining the discrepancy of the functions of SEMA5A, it was thus speculated that the cleaved extracellular domain and full-length of SEMA5A may carry out opposite functions in different cancer types. The alternative explanation is that receptor-ligand interactions generate simultaneous bidirectional signals (i.e., forward signaling and reverse signaling) with opposite functions (65-67). That is, the full-length of SEMA5A on the membrane may function as both a receptor and ligand to

generate simultaneous forward and reverse signals, whereas the cleaved extracellular domain may only initiate reverse signaling by serving as ligand for receptors on other cells. Therefore, it was hypothesized that these phenomena may mainly be due to different experimental settings and tumor types. Yet, further studies are warranted to explore the function of SEMA5A in different cancer types.

Finally, the functions of *SEMA5A* in lung adenocarcinoma were investigated by identifying the downregulated related genes using microarrays. Both pathway analysis and network analysis revealed that one function of *SEMA5A*-regulated genes was cell growth and proliferation (Fig. 4). Among these genes involved in growth and proliferation, a number of genes have been reported with similar functions in other types of cancer. For example, *ARRDC3* and *CASP1* were found to be upregulated in this study. *ARRDC3* has been reported to suppress breast carcinoma invasion (68). The downregulation of the expression of *CASP1* has been shown to result in the proliferation and invasion of breast cancer cells (69). In this study, the functions of SEMA5A were further validated in *in vitro* (Fig. 5) and *in vivo* (Fig. 6) experiments, demonstrating that SEMA5A truly plays a tumor-suppressive role in the proliferation and migration of lung adenocarcinoma cells. On the whole, the findings of this study may thus contribute to the development of novel therapeutic regimens for lung adenocarcinoma in the future.

Acknowledgements

The authors would like to thank Dr Melissa Stauffer for providing editorial assistance.

Funding

This study was supported by grants from the Ministry of Science and Technology (NSC 98-2320-B-002-044-MY3 and MOST 106-2320-B-002-016-MY3) and China Medical University (CMU107-TU-09).

Availability of data and materials

All data have been deposited in the Gene Expression Omnibus (GEO, GSE114578). The other data and materials are available upon request from the corresponding authors.

Authors' contributions

PHK, GL, YPS and LCL conceived and designed the experiments. PHK, GL and YPS performed the experiments. PHK, GL, YAC, MHT and EYC analyzed the data. MHT, EYC and LCL contributed reagents, materials and/or analysis tools. PHK, GL, YPS and LCL wrote the manuscript. All authors have reviewed and approved the final manuscript.

Ethics approval and consent to participate

This animal model followed protocols approved by the Institutional Animal Care and Use Committee of China Medical University and Hospital (animal protocol no. 2016-102).

Patient consent for publication

Not applicable.

Competing interests

The authors declare that they have no competing interests.

References

1. Zhang N, Wei X and Xu L: miR-150 promotes the proliferation of lung cancer cells by targeting P53. FEBS Lett 587: 2346-2351, 2013.
2. Jemal A, Bray F, Center MM, Ferlay J, Ward E and Forman D: Global cancer statistics. CA Cancer J Clin 61: 69-90, 2011.
3. Molina JR, Yang P, Cassivi SD, Schild SE and Adjei AA: Non-small cell lung cancer: Epidemiology, risk factors, treatment, and survivorship. Mayo Clin Proc 83: 584-594, 2008.
4. Siegel R, Ward E, Brawley O and Jemal A: Cancer statistics, 2011: The impact of eliminating socioeconomic and racial disparities on premature cancer deaths. CA Cancer J Clin 61: 212-236, 2011.
5. Boyero L, Sánchez-Palencia A, Miranda-León MT, Hernández-Escobar F, Gómez-Capilla JA and Fárez-Vidal ME: Survival, classifications, and desmosomal plaque genes in non-small cell lung cancer. Int J Med Sci 10: 1166-1173, 2013.
6. Shaoyan X, Juanjuan Y, Yalan T, Ping H, Jianzhong L and Qinian W: Downregulation of EIF4A2 in non-small-cell lung cancer associates with poor prognosis. Clin Lung Cancer 14: 658-665, 2013.
7. Vendetti FP and Rudin CM: Epigenetic therapy in non-small-cell lung cancer: Targeting DNA methyltransferases and histone deacetylases. Expert Opin Biol Ther 13: 1273-1285, 2013.
8. Adams RH, Betz H and Püschel AW: A novel class of murine semaphorins with homology to thrombospondin is differentially expressed during early embryogenesis. Mech Dev 57: 33-45, 1996.
9. Capparuccia L and Tamagnone L: Semaphorin signaling in cancer cells and in cells of the tumor microenvironment-two sides of a coin. J Cell Sci 122: 1723-1736, 2009.
10. Christensen C, Ambartsumian N, Gilestro G, Thomsen B, Comoglio P, Tamagnone L, Guldberg P and Lukanidin E: Proteolytic processing converts the repelling signal Sema3E into an inducer of invasive growth and lung metastasis. Cancer Res 65: 6167-6177, 2005.
11. Adams RH, Lohrum M, Klostermann A, Betz H and Püschel AW: The chemorepulsive activity of secreted semaphorins is regulated by furin-dependent proteolytic processing. EMBO J 16: 6077-6086, 1997.
12. Hattori M, Osterfield M and Flanagan JG: Regulated cleavage of a contact-mediated axon repellent. Science 289: 1360-1365, 2000.
13. Esselens C, Malapeira J, Colome N, Casal C, Rodríguez-Manzaneque JC, Canals F and Arribas J: The cleavage of semaphorin 3C induced by ADAMTS1 promotes cell migration. J Biol Chem 285: 2463-2473, 2010.
14. Browne K, Wang W, Liu RQ, Piva M and O'Connor TP: Transmembrane semaphorin5B is proteolytically processed into a repulsive neural guidance cue. J Neurochem 123: 135-146, 2012.
15. Potiron VA, Roche J and Drabkin HA: Semaphorins and their receptors in lung cancer. Cancer Lett 273: 1-14, 2009.
16. Chedotal A, Kerjan G and Moreau-Fauvarque C: The brain within the tumor: New roles for axon guidance molecules in cancers. Cell Death Differ 12: 1044-1056, 2005.
17. Behar O, Golden JA, Mashimo H, Schoen FJ and Fishman MC: Semaphorin III is needed for normal patterning and growth of nerves, bones and heart. Nature 383: 525-528, 1996.
18. Hall KT, Boumsell L, Schultze JL, Boussiotis VA, Dorfman DM, Cardoso AA, Bensussan A, Nadler LM and Freeman GJ: Human CD100, a novel leukocyte semaphorin that promotes B-cell aggregation and differentiation. Proc Natl Acad Sci USA 93: 11780-11785, 1996.
19. Miao HQ, Soker S, Feiner L, Alonso JL, Raper JA and Klagsbrun M: Neuropilin-1 mediates collapsin-1/semaphorin III inhibition of endothelial cell motility: Functional competition of collapsin-1 and vascular endothelial growth factor-165. J Cell Biol 146: 233-242, 1999.

20. Christensen CR, Klingelhofer J, Tarabykina S, Hulgaard EF, Kramerov D and Lukanidin E: Transcription of a novel mouse semaphorin gene, M-semaH, correlates with the metastatic ability of mouse tumor cell lines. Cancer Res 58: 1238-1244, 1998.
21. Chen R, Zhuge X, Huang Z, Lu D, Ye X, Chen C, Yu J and Lu G: Analysis of SEMA3B methylation and expression patterns in gastric cancer tissue and cell lines. Oncol Rep 31: 1211-1218, 2014.
22. Gao X, Tang C, Shi W, Feng S, Qin W, Jiang T and Sun Y: Semaphorin-3F functions as a tumor suppressor in colorectal cancer due to regulation by DNA methylation. Int J Clin Exp Pathol 8: 12766-12774, 2015.
23. Kruger RP, Aurandt J and Guan KL: Semaphorins command cells to move. Nat Rev Mol Cell Biol 6: 789-800, 2005.
24. Nagai H, Sugito N, Matsubara H, Tatematsu Y, Hida T, Sekido Y, Nagino M, Nimura Y, Takahashi T and Osada H: CLCP1 interacts with semaphorin 4B and regulates motility of lung cancer cells. Oncogene 26: 4025-4031, 2007.
25. Nasarre P, Kusy S, Constantin B, Castellani V, Drabkin HA, Bagnard D and Roche J: Semaphorin SEMA3F has a repulsing activity on breast cancer cells and inhibits E-cadherin-mediated cell adhesion. Neoplasia 7: 180-189, 2005.
26. Castro-Rivera E, Ran S, Thorpe P and Minna JD: Semaphorin 3B (SEMA3B) induces apoptosis in lung and breast cancer, whereas VEGF165 antagonizes this effect. Proc Natl Acad Sci USA 101: 11432-11437, 2004.
27. Tomizawa Y, Sekido Y, Kondo M, Gao B, Yokota J, Roche J, Drabkin H, Lerman MI, Gazdar AF and Minna JD: Inhibition of lung cancer cell growth and induction of apoptosis after reexpression of 3p21.3 candidate tumor suppressor gene SEMA3B. Proc Natl Acad Sci USA 98: 13954-13959, 2001.
28. Brambilla E, Constantin B, Drabkin H and Roche J: Semaphorin SEMA3F localization in malignant human lung and cell lines: A suggested role in cell adhesion and cell migration. Am J Pathol 156: 939-950, 2000.
29. Lu TP, Tsai MH, Lee JM, Hsu CP, Chen PC, Lin CW, Shih JY, Yang PC, Hsiao CK, Lai LC and Chuang EY: Identification of a novel biomarker, SEMA5A, for non-small cell lung carcinoma in nonsmoking women. Cancer Epidemiol Biomarkers Prev 19: 2590-2597, 2010.
30. Kolodkin AL, Matthes DJ and Goodman CS: The semaphorin genes encode a family of transmembrane and secreted growth cone guidance molecules. Cell 75: 1389-1399, 1993.
31. Bahri SM, Chia W and Yang X: Characterization and mutant analysis of the Drosophila sema 5c gene. Dev Dyn 221: 322-330, 2001.
32. Gras C, Eiz-Vesper B, Jaimes Y, Immenschuh S, Jacobs R, Witte T, Blasczyk R and Figueiredo C: Secreted semaphorin 5A activates immune effector cells and is a biomarker for rheumatoid arthritis. Arthritis Rheumatol 66: 1461-1471, 2014.
33. Arribas J and Borroto A: Protein ectodomain shedding. Chem Rev 102: 4627-4638, 2002.
34. Simmons AD, Overhauser J and Lovett M: Isolation of cDNAs from the Cri-du-chat critical region by direct screening of a chromosome 5-specific cDNA library. Genome Res 7: 118-127, 1997.
35. Mosca-Boidron AL, Gueneau L, Huguet G, Goldenberg A, Henry C, Gigot N, Pallesi-Pocachard E, Falace A, Duplomb L, Thevenon J, *et al*: A de novo microdeletion of SEMA5A in a boy with autism spectrum disorder and intellectual disability. Eur J Hum Genet 24: 838-843, 2016.
36. Sadanandam A, Rosenbaugh EG, Singh S, Varney M and Singh RK: Semaphorin 5A promotes angiogenesis by increasing endothelial cell proliferation, migration, and decreasing apoptosis. Microvasc Res 79: 1-9, 2010.
37. Sadanandam A, Varney ML, Singh S, Ashour AE, Moniaux N, Deb S, Lele SM, Batra SK and Singh RK: High gene expression of semaphorin 5A in pancreatic cancer is associated with tumor growth, invasion and metastasis. Int J Cancer 127: 1373-1383, 2010.
38. Sadanandam A, Varney ML, Kinarsky L, Ali H, Mosley RL and Singh RK: Identification of functional cell adhesion molecules with a potential role in metastasis by a combination of in vivo phage display and in silico analysis. OMICS 11: 41-57, 2007.
39. Pan G, Zhang X, Ren J, Lu J, Li W, Fu H, Zhang S and Li J: Semaphorin 5A, an axon guidance molecule, enhances the invasion and metastasis of human gastric cancer through activation of MMP9. Pathol Oncol Res 19: 11-18, 2013.
40. Saxena S, Purohit A, Varney ML, Hayashi Y and Singh RK: Semaphorin-5A maintains epithelial phenotype of malignant pancreatic cancer cells. BMC Cancer 18: 1283, 2018.
41. Li X and Lee AY: Semaphorin 5A and plexin-B3 inhibit human glioma cell motility through RhoGDIα-mediated inactivation of Rac1 GTPase. J Biol Chem 285: 32436-32445, 2010.
42. Li X, Law JW and Lee AY: Semaphorin 5A and plexin-B3 regulate human glioma cell motility and morphology through Rac1 and the actin cytoskeleton. Oncogene 31: 595-610, 2012.
43. Lin CY, Chen HJ, Huang CC, Lai LC, Lu TP, Tseng GC, Kuo TT, Kuok QY, Hsu JL, Sung SY, *et al*: ADAM9 promotes lung cancer metastases to brain by a plasminogen activator-based pathway. Cancer Res 74: 5229-5243, 2014.
44. Livak KJ and Schmittgen TD: Analysis of relative gene expression data using real-time quantitative PCR and the 2(-Delta Delta C(T)) method. Methods 25: 402-408, 2001.
45. Feinberg AP and Tycko B: The history of cancer epigenetics. Nat Rev Cancer 4: 143-153, 2004.
46. Jones PA and Baylin SB: The fundamental role of epigenetic events in cancer. Nat Rev Genet 3: 415-428, 2002.
47. Lin HC, Yeh CC, Chao LY, Tsai MH, Chen HH, Chuang EY and Lai LC: The hypoxia-responsive lncRNA NDRG-OT1 promotes NDRG1 degradation via ubiquitin-mediated proteolysis in breast cancer cells. Oncotarget 9: 10470-10482, 2018.
48. The PONES: Correction: Online survival analysis software to assess the prognostic value of biomarkers using transcriptomic data in non-small-cell lung cancer. PLoS One 9: e111842, 2014.
49. Győrffy B, Surowiak P, Budczies J and Lánczky A: Online survival analysis software to assess the prognostic value of biomarkers using transcriptomic data in non-small-cell lung cancer. PLoS One 8: e82241, 2013.
50. Bild AH, Yao G, Chang JT, Wang Q, Potti A, Chasse D, Joshi MB, Harpole D, Lancaster JM, Berchuck A, *et al*: Oncogenic pathway signatures in human cancers as a guide to targeted therapies. Nature 439: 353-357, 2006.
51. Director's Challenge Consortium for the Molecular Classification of Lung Adenocarcinoma; Shedden K, Taylor JM, Enkemann SA, Tsao MS, Yeatman TJ, Gerald WL, Eschrich S, Jurisica I, Giordano TJ, *et al*: Gene expression-based survival prediction in lung adenocarcinoma: A multi-site, blinded validation study. Nat Med 14: 822-827, 2008.
52. Selamat SA, Chung BS, Girard L, Zhang W, Zhang Y, Campan M, Siegmund KD, Koss MN, Hagen JA, Lam WL, *et al*: Genome-scale analysis of DNA methylation in lung adenocarcinoma and integration with mRNA expression. Genome Res 22: 1197-1211, 2012.
53. Roche J, Boldog F, Robinson M, Robinson L, Varella-Garcia M, Swanton M, Waggoner B, Fishel R, Franklin W, Gemmill R and Drabkin H: Distinct 3p21.3 deletions in lung cancer and identification of a new human semaphorin. Oncogene 12: 1289-1297, 1996.
54. Xiang RH, Hensel CH, Garcia DK, Carlson HC, Kok K, Daly MC, Kerbacher K, van den Berg A, Veldhuis P, Buys CH and Naylor SL: Isolation of the human semaphorin III/F gene (SEMA3F) at chromosome 3p21, a region deleted in lung cancer. Genomics 32: 39-48, 1996.
55. Pan G, Lv H, Ren H, Wang Y, Liu Y, Jiang H and Wen J: Elevated expression of semaphorin 5A in human gastric cancer and its implication in carcinogenesis. Life Sci 86: 139-144, 2010.
56. Wang DG, Yousif NG, Sadiq AM, Schilling MM and Danielson X: Critical role of SEMA5A expression in invasion and metastasis of ovarian cancer cell. Am J Biomed 2: 292-305, 2014.
57. Saxena S, Hayashi Y, Wu L, Awaji M, Atri P, Varney ML, Purohit A, Rachagani S, Batra SK and Singh RK: Pathological and functional significance of Semaphorin-5A in pancreatic cancer progression and metastasis. Oncotarget 9: 5931-5943, 2017.
58. Baylin SB, Esteller M, Rountree MR, Bachman KE, Schuebel K and Herman JG: Aberrant patterns of DNA methylation, chromatin formation and gene expression in cancer. Hum Mol Genet 10: 687-692, 2001.
59. Lenka G, Tsai MH, Hsiao JH, Lai LC and Chuang EY: Overexpression of methylation-driven DCC suppresses proliferation of lung cancer cells. Translational Cancer Res 5: 169-175, 2016.
60. Lenka G, Tsai MH, Lin HC, Hsiao JH, Lee YC, Lu TP, Lee JM, Hsu CP, Lai LC and Chuang EY: Identification of methylation-driven, differentially expressed STXBP6 as a novel biomarker in lung adenocarcinoma. Sci Rep 7: 42573, 2017.

61. Baumgart A, Seidl S, Vlachou P, Michel L, Mitova N, Schatz N, Specht K, Koch I, Schuster T, Grundler R, *et al*: ADAM17 regulates epidermal growth factor receptor expression through the activation of Notch1 in non-small cell lung cancer. Cancer Res 70: 5368-5378, 2010.
62. Sharma A, Bender S, Zimmermann M, Riesterer O, Broggini-Tenzer A and Pruschy MN: Secretome signature identifies ADAM17 as novel target for radiosensitization of non-small cell lung cancer. Clin Cancer Res 22: 4428-4439, 2016.
63. Lv X, Li Y, Qian M, Ma C, Jing H, Wen Z and Qian D: ADAM17 silencing suppresses the migration and invasion of non-small cell lung cancer. Mol Med Rep 9: 1935-1940, 2014.
64. Sadanandam A, Sidhu SS, Wullschleger S, Singh S, Varney ML, Yang CS, Ashour AE, Batra SK and Singh RK: Secreted semaphorin 5A suppressed pancreatic tumour burden but increased metastasis and endothelial cell proliferation. Br J Cancer 107: 501-507, 2012.
65. Hamada K, Oike Y, Ito Y, Maekawa H, Miyata K, Shimomura T and Suda T: Distinct roles of ephrin-B2 forward and EphB4 reverse signaling in endothelial cells. Arterioscler Thromb Vasc Biol 23: 190-197, 2003.
66. Zhang H, Yan D, Shi X, Liang H, Pang Y, Qin N, Chen H, Wang J, Yin B, Jiang X, *et al*: Transmembrane TNF-alpha mediates 'forward' and 'reverse' signaling, inducing cell death or survival via the NF-kappaB pathway in Raji Burkitt lymphoma cells. J Leukoc Biol 84: 789-797, 2008.
67. Godenschwege TA, Hu H, Shan-Crofts X, Goodman CS and Murphey RK: Bi-directional signaling by Semaphorin 1a during central synapse formation in Drosophila. Nat Neurosci 5: 1294-1301, 2002.
68. Arakaki AKS, Pan WA, Lin H and Trejo J: The alpha-arrestin ARRDC3 suppresses breast carcinoma invasion by regulating G protein-coupled receptor lysosomal sorting and signaling. J Biol Chem 293: 3350-3362, 2018.
69. Sun Y and Guo Y: Expression of Caspase-1 in breast cancer tissues and its effects on cell proliferation, apoptosis and invasion. Oncol Lett 15: 6431-6435, 2018.